

EFFICIENT STRESS RETURN ALGORITHMS USING ENERGY-MAPPED STRESS SPACE

Roger S Crouch* and Harm Askes†

* School of Engineering, University of Durham,
South Road, Durham DH1 3LE, UK
e-mail: r.s.crouch@durham.ac.uk

† Department of Civil & Structural Engineering, University of Sheffield
Mappin Street, Sheffield S1 3JD, UK
e-mail: h.askses@sheffield.ac.uk

Key words: Closest Point Projection, Energy-Mapped Stresses

Summary. *This paper makes use of energy-mapped stress measures when using Closest-Point Projection stress return algorithms in computational plasticity. Operating with this transformed space allows the corrective plastic return path to become the shortest Euclidean distance between the predictive elastic trial stress and the converged solution on the yield surface (not generally the case in conventional stress space). Furthermore, the graphical interpretation afforded by this mapping suggests both parameter reduction and appropriate Newton-Raphson initiation states to be selected, allowing efficient iterative algorithms to be developed when closed-form solutions are not possible.*

1 CPP STRESS RETURN

Stress return algorithms are central to computational plasticity. If elastic trial stresses are found to be outside the yield surface, then they must be projected back onto the yield surface, such that consistency is satisfied at the final *return* stress state. The latter is found by locating the point on the yield surface that is closest to those trial stresses. The algorithm is accordingly denoted a *Closest-Point Projection* (or CPP, [1]). For complicated yield surfaces, the CPP leads to a set of nonlinear equations such that a numerical solution strategy must be pursued. In most finite element codes the CPP method is combined with a consistent linearisation and a Newton-Raphson iterative scheme.

Unfortunately, the term CPP is somewhat misleading, since the return stress is *not* closest to the trial stress in a conventional Euclidean sense. Rather, it is closest in one particular metric; namely the *elastic energy metric* [1]. It is, however, possible to identify another stress tensor such that the CPP is indeed the closest point in a standard Euclidean sense. This new *energy-mapped* stress tensor is defined in the next section.

Carrying out the stress return in this alternative space offers some advantages:

1. By reducing the task to finding the Euclidean closest point, it clarifies which classes of yield functions support analytical returns. Closed-form solutions exist for those

functions expressible in a polynomial form of order less than 5 (for example, isotropic surfaces comprising combinations of conic meridional and circular deviatoric sections, or multi-planar Tresca/Mohr-Coulomb surfaces).

2. Use can be made of certain geometric considerations, by which the number of nonlinear equations to be solved in a stress return can be reduced. Guided by the simpler geometry in the energy-mapped stress space, we have found that for certain yield functions parametric reduction is possible and non-convergence through jumping to inadmissible stress states can be avoided. In the example given below, a single parameter is all that is required.
3. In turn, reducing the number of variables in the nonlinear equations eases the task of identifying a proper initialization of the Newton-Raphson procedure within the radius of convergence allowing quadratic convergence.
4. Finally, the clear graphical interpretation can be of value when coding and debugging advanced constitutive models. Difficulties associated with regions of significant yield-surface curvature can be revealed, and overcome, if the CPP solutions are compared with simple local geometric searches.

2 THE (ELASTIC) ENERGY-MAPPED STRESS TENSOR

The CPP method may be viewed as providing a discrete solution to a constrained optimisation problem whereby the plastic corrector stresses are projected orthogonally to the yield surface in the $[\mathbf{G}]^{-1}$ metric. Armero and Pérez-Foguet [2] note that the Hessian

$$[\mathbf{G}] = \begin{bmatrix} \psi_{,\varepsilon^e\varepsilon^e} & -\psi_{,\varepsilon^eq} \\ -\psi_{,q\varepsilon^e} & \psi_{,qq} \end{bmatrix} \quad (1)$$

where ψ is the stored energy function and $\{q\}$ represent strain-like hardening variables. In the case of perfect plasticity, $[\mathbf{G}] = [\mathbf{D}^e]$. This implies that the correct path is the one that minimizes the incremental elastic work $|\{\Delta\sigma\}^T[\mathbf{D}^e]^{-1}\{\Delta\sigma\}/2|$ while simultaneously satisfying the consistency condition $f = 0$. We identify the energy-mapped stresses $\{\varsigma\}$ from $\{\varsigma\}^T\{\varsigma\} = E\{\sigma\}^T[\mathbf{D}^e]^{-1}\{\sigma\}$. (The factor E enables σ and ς to be plotted together.) For isotropic elasticity we define $\{\varsigma\} = [T]\{\sigma\}$ where

$$[T] = \begin{bmatrix} t_1 & t_2 & t_2 & 0 & 0 & 0 \\ t_2 & t_1 & t_2 & 0 & 0 & 0 \\ t_2 & t_2 & t_1 & 0 & 0 & 0 \\ 0 & 0 & 0 & t_3 & 0 & 0 \\ 0 & 0 & 0 & 0 & t_3 & 0 \\ 0 & 0 & 0 & 0 & 0 & t_3 \end{bmatrix} \quad \text{and} \quad \begin{aligned} t_1 &= \sqrt{1 - \frac{2(2-\nu-2\sqrt{1-\nu-2\nu^2})}{9}} \\ t_2 &= -\sqrt{\frac{1-(t_1)^2}{2}} \\ t_3 &= \sqrt{2(1+\nu)} \end{aligned} \quad (2)$$

In conventional stress space (for pressure-sensitive yield surfaces) it is only when $\nu = 0$ (or when the trial stress is purely hydrostatic) that the return path from the trial state will be parallel to the surface normal. In the transformed space, the return path is *always* in the direction of the surface normal. Figure 1 (on the right) shows two views of the same closed yield surface. The upper image corresponds to the plot in conventional stress space; the lower to the energy-mapped space. The effect of the mapping is to hydrostatically squash and deviatorically stretch the yield surface. For example, in the case of a cohesionless isotropic Drucker-Prager model, the cone *gradient*, $\alpha = \frac{\rho}{\xi}$ increases by the factor $(t_1 - t_2)/(t_1 + 2t_2)$.

3 CPP RETURN FOR 3-PARAMETER WILLAM-WARNKE MODEL

We now consider a pressure-dependant yield surface where the meridional sections are linear but the deviatoric cross-sections are defined in terms of segments of ellipses [3]. It can be shown that the Lode angle corresponding to the converged solution is given by finding the stationary (maximum) value of the scalar function

$$\frac{1 + \eta \cdot \alpha \cdot r \cos(\theta - \phi)}{\sqrt{1 + (\alpha \cdot r)^2}} \quad (3)$$

where η is the stress ratio ($\rho_\varsigma/\xi_\varsigma$) of the trial stress state, α is the slope of the compression meridian (again in terms of $\rho_\varsigma/\xi_\varsigma$), θ is the Lode angle corresponding to the trial stress state and ϕ is the Lode angle corresponding to the solution. ξ_ς and ρ_ς are respectively the cylindrical hydrostatic and deviatoric invariants of ς . $r(\phi)$ describes the deviatoric elliptic shape function. Maximization and linearisation of (3) leads to a scalar equation in terms of the single unknown ϕ . The upper left plot in Figure 1 shows g functions for eleven regularly spaced trial states where $-\pi/6 \leq \theta \leq \pi/6$. Two iterations of the N-R scheme are shown (A-D) for the case $\theta = 0$. In the lower left plot, the ϕ solutions for all θ are illustrated, together with the number of iterations required to reach convergence ($g/|\hat{g}| < 10^{-9}$). That plot also identifies the initial values of ϕ given by the bi-linear upper boundary obtained from the tangents at either end of the range. The solution converges monotonically, with a maximum number of iterations of 5.

REFERENCES

- [1] Simo, J C and Hughes, T J R, *Computational Inelasticity*, Springer, 1998.
- [2] Armero, F and Pérez-Foguet, A, *On the Formulation of Closest-Point Projection Algorithms in Elastoplasticity. Part I: The Variational Structure*, University of Berkeley, Department of Civil & Environmental Engineering Report, 1999.
- [3] Willam, K J and Warnke, E P, Constitutive model for triaxial behavior of concrete, *Proc IABSE Seminar on Concrete Structures Subjected to Triaxial Stresses*, 19, ISMES, Bergamo, Italy, 1975.

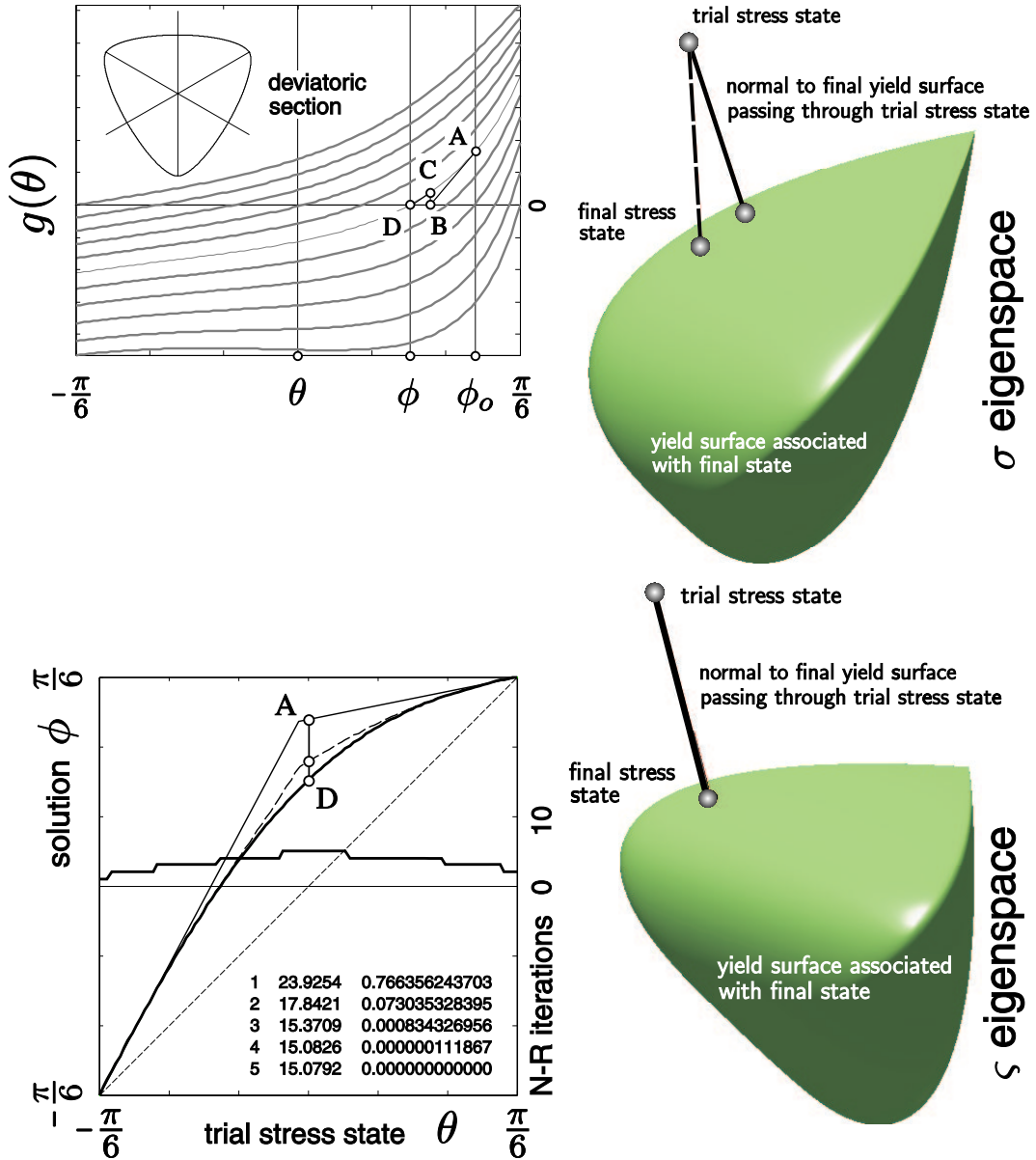


Figure 1: Top right; closed pressure-sensitive surface in conventional stress space. Bottom right; the same yield state in ζ space. Top left; variation in g with respect to ϕ for different θ when $\eta = 10\alpha$, plus N-R iterations for the case $\theta = 0$. Bottom left; ϕ solutions for all θ (of which D is just one), plus number of iterations required. The path from the initial state at A to the solution at D applies to the case $\theta = 0$ when $\eta = 10\alpha$. The values of g (together with ϕ , in degrees) for each iteration exhibit a quadratic rate of convergence.